Journal of Inclusion Phenomena **6** (1988), 15–30.

Separation of Phenol and Cresols by Crystalline Complexation with 1,1-Di(*p*-hydroxyphenyl)cyclohexane, and Crystal Structure Analyses of the Complexes

ISRAEL GOLDBERG* and ZAFRA STEIN
School of Chemistry, Sackler Faculty of Exact Sciences, Tel-Aviv University, 69978 Ramat-Aviv, Israel

KOICHI TANAKA and FUMIO TODA*
Department of Industrial Chemistry, Faculty of Engineering, Ehime University, Matsuyama 790, Japan

(Received: 12 February 1987)

Abstract. This paper is concerned with 1 : 1 inclusion complexes of the 1,1-di(*p*-hydroxyphenyl)cyclohexane host with either phenol or one of the cresol derivatives as guest. Selectivity studies showed preferential complexation with a guest according to the sequence: *m*-cresol > *p*-cresol > phenol > *o*-cresol. Crystallographic analyses of the four complexes revealed isomorphous structures [crystal data for the phenol complex: $a = 6.232$, $b = 10.849$, $c = 14.845$ Å, $\alpha = 95.69$, $\beta = 93.49$, $\gamma = 104.31°$, space group $P\bar{1}$, $Z = 2$]. The intermolecular arrangements are characterized by layers of efficiently hydrogen bonded entities (host-to-host, host-to-guest and guest-to-host) parallel to *ab*, every OH group being involved in two H-bonds. Organization of the layers along *c* is stabilized by weak dispersion forces, thus being most sensitive to structural variation of the guest component. The observed features of selectivity upon crystalline complexation are related to differences in topological complementarity between the constituents of each structure.

Key words: Molecular separation by crystalline complexation, coordinato-clathrates, inclusion complexes.

Supplementary Data relating to this article are deposited with the British Library as Supplementary Publication No. SUP 82052 (4 pages).

1. Introduction

The separation of cresols from the cresol mixture which is obtained from coal tar has long been an important subject of chemistry. Especially, separation of *m*- (**2**, b.p. 202.0 °C) and *p*-cresol (**3**, b.p. 201.8 °C) is the most important but difficult problem because of their very close boiling points. Several successful applications of the lattice inclusion phenomena to problems of molecular separation have been reported in the literature in recent years [1–3]. They indicated that both functional as well as topological complementarity between host and guest is essential for gaining a better selectivity in the process of clathrate formation. As part of our continuing interest in this field we attempted a separation of one component from a mixture of two cresols or of cresol and phenol by crystalline complexation with 1,1-di(*p*-hydroxyphenyl)cyclohexane (**5**) [4]. The hydrocarbon framework of **5** provides the bulk of the host lattice,

* Author for correspondence.

while the two hydroxyls attached to it from both sides act as 'functional sensors'. The ratio of products obtained by distilling the complex derived from **5** and a 1 : 1 mixture of two components showed which component is more strongly included in the crystal lattice. The results disclosed a sequence of preferential complex formation between **5** and a phenol derivative in the order **2** > **3** > **4** > **1**. This observation suggested a possibility of *m*-cresol isolation from a cresol mixture, and we have succeeded in fact to isolate 98.5% pure **2** in 55% yield. Crystallographic analysis of the inclusion complexes was needed in order to relate the questions of why *m*-cresol is cocrystallized with **5** most easily, and why the inclusion ability of the other phenols follows the above sequence, to the structural characteristics of the corresponding complexes.

In the current investigation we were able to obtain the following crystalline complexes, analyze their detailed structure, and describe the interaction pattern between the various constituents.

I. 1 : 1 $C_{18}H_{20}O_2$ **(5)** + C_7H_8O **(1)**; **II.** 1 : 1 **(5)** + **(2)**;
III. 1 : 1 **(5)** + **(3)**; **IV.** 1 : 1 **(5)** + C_6H_6O **(4)**

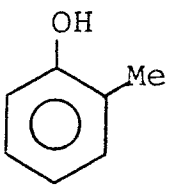

1

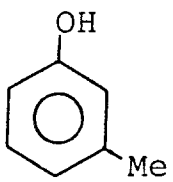

2

3

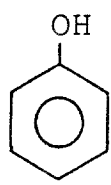

4

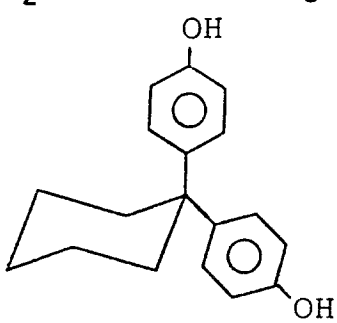

5

2. Experimental

General procedure for the separation of two cresols or of phenol and cresol. Equimolar amounts of two cresols (or phenol and cresol) and **5** were dissolved in ethylacetate by heating. Then, the solution was kept at room temperature for 12 h to give a 1 : 1 complex as colorless crystals. Heating of the complex at 200 °C under 20 mmHg gave a mixture of two cresols (or phenol and cresol). The ratio of the two components was determined by gas chromatography.

Separation of one component in a pure state is not difficult. The crude complex can be purified by recrystallization from ethyl acetate to give the pure complex of one component, which upon heating in vacuo gives pure cresol or phenol. For

example, a 1 : 1 mixture of **2** and **3** (2.16 g, 10.0 mmol each) and **5** (2.68 g, 10.0 mmol) was dissolved in ethylacetate (7 ml) by heating. Slow crystallization of the solution at room temperature gave colorless prisms (2.68 g). Heating of the complex at 200 °C under 20 mm Hg resulted in a 65.9 : 34.1 mixture of **2** and **3** (0.76 g). Recrystallization of the above complex from ethylacetate led to a 1 : 1 complex of pure **2** and **5**, which upon distillation gave 99.8% pure **2** (0.35 g, 32%).

The composition of the cresol mixture from coal tar is **2** (54.1%), **3** (27.3%), 1 and 2,6-dimethylphenol (4.0%), and 2,4-dimethylphenol and 2,5-dimethylphenol (14.4%).

Crystal structure analyses. X-ray diffraction data were measured at 18 °C on a CAD4 diffractometer equipped with a graphite monochromator, using Mo$K\alpha$ ($\lambda = 0.7107$ Å) radiation and the ω-2θ scan technique. The four compounds crystallized in an isomorphous manner in space group $P\bar{1}$ with two entities of the 1 : 1 complex in the unit cell. The cell constants and pertinent details of the experimental conditions are summarized in Table I. All intensity data sets were recorded at a constant 2°min^{-1} scan rate out to $2\theta_{max} = 50°$. Possible deterioration of the analyzed crystals was tested by measuring frequently the intensities of three standard reflections; for compounds **II–IV** it was found to be negligible during the measurements. The standard intensities monitored for complex **I** exhibited however a linear decrease as a function of time, which required an appropriate correction of this set of data. All intensities were corrected for Lorentz and polarization effects and background counts, but not for absorption and secondary extinction. Final refinements were based only on those observations that satisfied the condition $F_0^2 > 3\sigma(F_0^2)$.

The isomorphous crystal structures were solved by a combination of direct methods (MULTAN 80) [5] and Fourier techniques. Extensive use of the latter was made to locate the different phenolic guests within the four similar lattices of the host. The refinements were carried out by large block least-squares (SHELX 76) [6], including the positional and anisotropic thermal parameters of the nonhydrogen

Table I. Summary of Crystal Data and Experimental Parameters

Compound	I	II	III	IV
Mol wt	376.5	376.5	376.5	362.5
a, Å	6.270(2)	6.250(2)	6.237(4)	6.232(3)
b, Å	10.907(4)	10.807(2)	10.856(3)	10.849(2)
c, Å	15.446(7)	15.490(2)	15.818(4)	14.845(3)
α, deg	92.87 (4)	98.11 (1)	99.29 (2)	95.69 (1)
β, deg	93.33 (3)	93.41 (2)	92.21 (3)	93.49 (3)
γ, deg	102.15 (4)	101.11 (2)	105.67 (3)	104.31 (3)
V, Å^3	1028.8	1012.3	1013.9	964.0
d_c, gcm^{-3}	1.215	1.235	1.233	1.249
μ, cm^{-1}	0.73	0.74	0.74	0.76
No. of unique data > 0	2288	3201	3098	3007
Data with $I > 3\sigma_I$	1011	2204	1865	1888
F(000), e	404	404	404	388
R	0.094	0.049	0.055	0.054
R_w	0.093	0.052	0.055	0.056
$\lvert\Delta\rho\rvert_{max}$, e Å^{-3}	0.41	0.35	0.34	0.26
GOF, e	1.29	1.61	1.55	1.06

atoms. Most hydrogens were introduced into the structure-factor computations in calculated positions (the methyl substituents being treated as rigid groups); those involved in hydrogen bonds in compounds **II–IV** were located directly in difference-Fourier maps. The hydroxyl H-atoms in **I** could not be located (see below). Least squares calculations were based on the experimental weights $[w = 1/\sigma^2(F_0)]$, the quantity minimized being $w(\Delta F)^2$.

Structures **II–IV** turned out to be perfectly ordered and well defined. Much less precise was the determination of structure **I**, due to a partial disorder exhibited by the *o*-cresol guest as well as the poor quality of the intensity data set obtained for this compound. This is well reflected in the relatively large parameters of thermal motion characterizing the individual atoms, the low percentage of strong reflections (poor diffraction), and correspondingly high e.s.d.s of the refined parameters which are several times larger in **I** than in the other compounds. In order to avoid unreasonable distortions of bond lengths and bond angles, the phenyl ring of *o*-cresol in **I** was refined as a rigid group with a constrained hexagonal geometry.

The final difference-Fourier maps of the four structures showed no indication of incorrectly placed or missing atoms; the highest peak and deepest trough range from 0.21 (in **IV**) to 0.33 e $Å^{-3}$ (in **I**) and from –0.26 (in **IV**) to –0.41 e $Å^{-3}$ (in **I**), respectively. The crystallographic atom labeling scheme used for compound **IV** is shown below. A similar scheme applies to complexes **I–III**, with the $—CH_3$ substituent in the various cresols being marked as C(28).

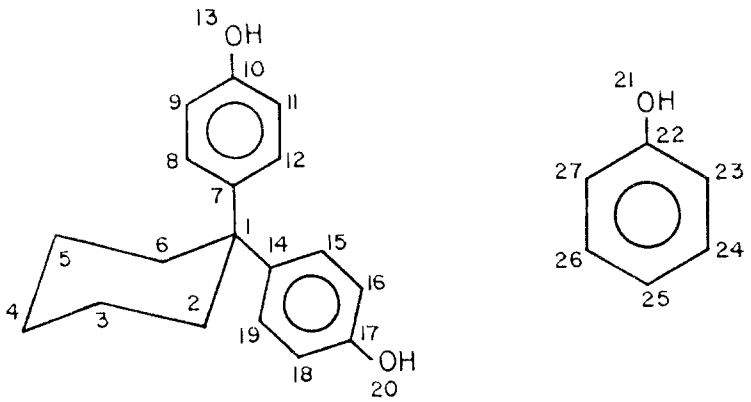

3. Results

Final atomic coordinates of the four compounds are listed in Tables II–V; lists of anisotropic thermal parameters have been deposited. The covalent bond lengths and bond angles obtained for the various molecules are compared in Table VI; they exhibit a good internal consistency and no extraordinary features. Moreover, the molecular conformation of the host is essentially the same in all compounds with only minor variations of the torsions about the cyclohexyl—phenyl bonds.

The basic crystal structure type observed in this study is represented by the structure of complex **IV** which includes the unsubstituted phenol; it is illustrated in Figure 1. This crystal structure can be best described as composed of 'layers' of hydrogen bonded species which lie parallel to the *ab* plane of the crystal. Within each such layer there is a characteristic pattern of hydrogen bonds as follows: Mole-

Table II. Atomic Coordinates and Isotropic Thermal Parameters of **I**. U_{eq} is one third of the trace of the orthogonalized U^{ij} tensor

Atom	*x/a*	*y/b*	*z/c*	U_{eq}
C(1)	−0.2402(19)	0.3074(10)	0.0926(7)	0.0433(28)
C(2)	−0.0966(19)	0.3083(10)	0.0168(7)	0.0437(28)
C(3)	−0.1667(19)	0.1949(10)	−0.0495(7)	0.0454(27)
C(4)	−0.4092(20)	0.1809(11)	−0.0823(7)	0.0540(29)
C(5)	−0.5542(19)	0.1782(11)	−0.0085(8)	0.0550(28)
C(6)	−0.4808(18)	0.2957(9)	0.0547(7)	0.0410(28)
C(7)	−0.2297(19)	0.1984(10)	0.1530(7)	0.0369(26)
C(8)	−0.3761(19)	0.1721(10)	0.2148(8)	0.0448(28)
C(9)	−0.3775(19)	0.0756(10)	0.2710(7)	0.0452(30)
C(10)	−0.2126(20)	0.0108(9)	0.2652(7)	0.0403(30)
C(11)	−0.0605(19)	0.0353(10)	0.2061(7)	0.0457(27)
C(12)	−0.0669(18)	0.1320(10)	0.1498(7)	0.0368(29)
O(13)	−0.1956(13)	−0.0864(7)	0.3191(5)	0.0569(25)
C(14)	−0.1603(18)	0.4293(10)	0.1496(7)	0.0382(27)
C(15)	0.0473(19)	0.4537(10)	0.1921(8)	0.0487(28)
C(16)	0.1275(19)	0.5643(10)	0.2424(7)	0.0518(29)
C(17)	0.0026(20)	0.6519(11)	0.2514(7)	0.0498(30)
C(18)	−0.2051(18)	0.6307(9)	0.2114(7)	0.0455(28)
C(19)	−0.2834(18)	0.5184(11)	0.1605(7)	0.0462(28)
O(20)	0.0918(13)	0.7630(7)	0.3027(5)	0.0619(25)
O(21)	−0.5431(13)	−0.1767(7)	0.4148(5)	0.0796(21)
C(22)	−0.5425(13)	−0.2511(8)	0.4852(5)	0.0791(29)
C(23)	−0.7253(13)	−0.3445(8)	0.4981(5)	0.1307(31)
C(24)	−0.7215(13)	−0.4207(8)	0.5678(5)	0.1586(31)
C(25)	−0.5349(13)	−0.4034(8)	0.6247(5)	0.1176(28)
C(26)	−0.3521(13)	−0.3101(8)	0.6117(5)	0.1022(31)
C(27)	−0.3559(13)	−0.2339(8)	0.5420(5)	0.1043(29)
C(28)	−0.1709(22)	−0.1351(14)	0.5339(10)	0.1521(30)
H(13)	−0.3529	−0.1142	0.3343	0.050
H(20)	−0.0617	0.7858	0.3085	0.050
H(21)	−0.6845	−0.2052	0.3857	0.050

The phenyl ring of *o*-cresol (C(22) through C(27)) was refined as a rigid group with constrained hexagonal geometry.

cules of the host (**5**) related to each other by translation along *b* interact through their terminal hydroxyl groups OH(13) and OH(20), with one hydroxyl acting as a proton donor to and the other as a proton acceptor from the neighboring moieties. The continuous chains of the host molecules thus formed are linked one to another along the *a* axis through the phenolic guest, utilizing the dual capacity of a hydroxyl group for H-bonding. Thus, every OH(13)···OH(20) hydrophilic site attracts two guests (displaced by *a*) one from below and one from above. Correspondingly, each phenol bridge between adjacent chains of host moieties stacked along *a*, donates its hydroxyl proton to one chain and provides an acceptor site for a proton from another chain. As illustrated schematically in Figure 2a, this results in a two-dimensional cross-linked array of hydrogen bonded entities which is characterized by the general pattern host–host–host–··· along *b* and guest–(host–host)–guest–(host–host)–··· along *a*. The geometric details of these interactions are summarized in Table VII.

On the other hand, crystal packing of the H-bonded 'layers' along *c* is stabilized by

Table III. Atomic Coordinates and Isotropic Thermal Parameters of **II**. U_{eq} is one third of the trace of the orthogonalized U^{ij} tensor

Atom	*x/a*	*y/b*	*z/c*	U_{eq}
C(1)	−0.2358(4)	0.3186(2)	0.0925(2)	0.0300(6)
C(2)	−0.0923(4)	0.3062(2)	0.0149(2)	0.0340(6)
C(3)	−0.1672(4)	0.1840(3)	−0.0509(2)	0.0403(6)
C(4)	−0.4064(5)	0.1687(3)	−0.0857(2)	0.0489(7)
C(5)	−0.5519(4)	0.1786(3)	−0.0111(2)	0.0452(6)
C(6)	−0.4727(4)	0.3040(2)	0.0516(2)	0.0365(6)
C(7)	−0.2241(4)	0.2169(2)	0.1524(2)	0.0298(5)
C(8)	−0.3739(4)	0.1993(2)	0.2148(2)	0.0354(6)
C(9)	−0.3624(4)	0.1162(3)	0.2741(2)	0.0381(7)
C(10)	−0.1978(4)	0.0476(2)	0.2717(2)	0.0325(7)
C(11)	−0.0460(4)	0.0625(2)	0.2115(2)	0.0366(6)
C(12)	−0.0596(4)	0.1469(2)	0.1523(2)	0.0343(7)
O(13)	−0.1889(3)	−0.0330(2)	0.3334(1)	0.0454(6)
C(14)	−0.1530(4)	0.4494(2)	0.1489(2)	0.0301(6)
C(15)	0.0561(4)	0.4784(2)	0.1931(2)	0.0367(6)
C(16)	0.1394(4)	0.5947(3)	0.2450(2)	0.0374(6)
C(17)	0.0131(4)	0.6865(2)	0.2546(2)	0.0365(7)
C(18)	−0.1951(4)	0.6610(3)	0.2118(2)	0.0411(6)
C(19)	−0.2752(4)	0.5440(3)	0.1597(2)	0.0378(6)
O(20)	0.0865(3)	0.8040(2)	0.3051(1)	0.0500(5)
O(21)	−0.5365(3)	−0.1538(2)	0.4061(1)	0.0633(5)
C(22)	−0.4725(4)	−0.2145(3)	0.4730(2)	0.0424(6)
C(23)	−0.2595(4)	−0.1849(3)	0.5105(2)	0.0482(6)
C(24)	−0.2050(5)	−0.2494(3)	0.5766(2)	0.0532(7)
C(25)	−0.3597(5)	−0.3406(3)	0.6044(2)	0.0510(6)
C(26)	−0.5742(5)	−0.3687(3)	0.5680(2)	0.0449(7)
C(27)	−0.6286(4)	−0.3042(3)	0.5013(2)	0.0449(6)
C(28)	−0.7446(5)	−0.4658(3)	0.5999(2)	0.0625(7)
H(13)	−0.0664	−0.0817	0.3206	0.050
H(20)	0.2271	0.8053	0.3391	0.050
H(21)	−0.3981	−0.1054	0.3797	0.050

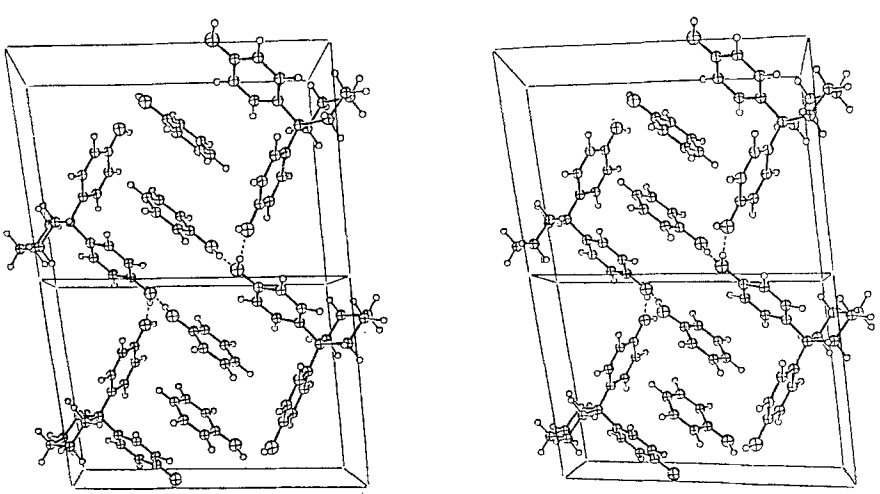

Fig. 1. Stereoview of the crystal structure of complex **IV**, approximately down the *a*-axis (*c* is horizontal).

Table IV. Atomic Coordinates and Isotropic Thermal Parameters of **III**. U_{eq} is one third of the trace of the orthogonalized U^{ij} tensor

Atom	*x/a*	*y/b*	*z/c*	U_{eq}
C(1)	−0.2460(5)	0.3251(3)	0.0947(2)	0.0305(9)
C(2)	−0.1022(5)	0.3178(3)	0.0178(2)	0.0339(8)
C(3)	−0.1833(6)	0.1910(3)	−0.0466(2)	0.0388(9)
C(4)	−0.4259(6)	0.1646(4)	−0.0800(2)	0.0475(10)
C(5)	−0.5705(6)	0.1705(4)	−0.0055(3)	0.0455(9)
C(6)	−0.4864(5)	0.2994(3)	0.0561(2)	0.0352(9)
C(7)	−0.2311(5)	0.2270(3)	0.1533(2)	0.0285(8)
C(8)	−0.3812(6)	0.2006(3)	0.2142(2)	0.0358(9)
C(9)	−0.3646(6)	0.1201(3)	0.2720(2)	0.0355(9)
C(10)	−0.1955(6)	0.0626(3)	0.2692(2)	0.0330(10)
C(11)	−0.0430(6)	0.0852(3)	0.2094(2)	0.0394(9)
C(12)	−0.0626(6)	0.1654(3)	0.1519(2)	0.0350(9)
O(13)	−0.1690(4)	−0.0179(2)	0.3261(2)	0.0466(8)
C(14)	−0.1603(5)	0.4617(3)	0.1500(2)	0.0299(9)
C(15)	0.0497(6)	0.5002(3)	0.1943(2)	0.0381(9)
C(16)	0.1347(6)	0.6205(3)	0.2455(2)	0.0416(9)
C(17)	0.0094(6)	0.7075(3)	0.2548(2)	0.0361(9)
C(18)	−0.2001(6)	0.6726(3)	0.2115(2)	0.0382(9)
C(19)	−0.2819(6)	0.5513(3)	0.1596(2)	0.0354(9)
O(20)	0.0977(4)	0.8271(2)	0.3068(2)	0.0497(8)
O(21)	−0.5232(4)	−0.1069(2)	0.4120(2)	0.0497(7)
C(22)	−0.5205(6)	−0.1901(3)	0.4688(2)	0.0396(9)
C(23)	−0.3205(6)	−0.1864(4)	0.5088(3)	0.0567(10)
C(24)	−0.3126(7)	−0.2716(4)	0.5647(3)	0.0641(10)
C(25)	−0.5009(8)	−0.3600(4)	0.5813(2)	0.0606(9)
C(26)	−0.7009(7)	−0.3591(4)	0.5420(3)	0.0612(9)
C(27)	−0.7128(6)	−0.2758(4)	0.4861(2)	0.0482(9)
C(28)	−0.4944(8)	−0.4555(4)	0.6402(3)	0.0895(11)
H(13)	−0.2971	−0.0381	0.3633	0.050
H(20)	−0.0175	0.8853	0.3045	0.050
H(21)	−0.6798	−0.1413	0.3729	0.050

weak van der Waals forces. The interlayer arrangement is shown in Figure 2b; it is characterized by a convenient steric fit between the convex and the concave surfaces of adjacent layers, which are related to each other by inversion. For example, the phenol guest attached to the top of one layer fits in between two other phenols located on the bottom of a neighboring layer. A similar complementarity is achieved between the cyclohexyl sides of adjacent layers (Figure 2b). All inter-layer distances in **IV** are equal to or larger than the sum of the corresponding van der Waals atomic radii; the shortest nonbonding contact is between two phenyl carbons at C(8) ··· C(25) = 3.492 Å.

The crystal structures of compounds **I**, **II** and **III** containing a cresol derivative instead of phenol as guest conform to the same structural model. They also consist of similar two-dimensional networks of efficiently H-bonded molecules which are aligned parallel to the *ab* plane of the crystal, their packing along *c* being stabilized by van der Waals interactions. The isomorphous appearance of these structures can be appreciated from Figures 3, 4 and 5, respectively, illustrating the intermolecular

Table V. Atomic Coordinates and Isotropic Thermal Parameters of **IV**. U_{eq} is one third of the trace of the orthogonalized U^{ij} tensor

Atom	*x/a*	*y/b*	*z/c*	U_{eq}
C(1)	−0.2419(5)	0.3133(3)	0.0978(2)	0.0374(7)
C(2)	−0.0999(5)	0.3104(3)	0.0165(2)	0.0417(7)
C(3)	−0.1791(5)	0.1899(3)	−0.0520(2)	0.0472(7)
C(4)	−0.4190(5)	0.1704(3)	−0.0868(2)	0.0552(8)
C(5)	−0.5631(5)	0.1712(3)	−0.0084(2)	0.0519(7)
C(6)	−0.4816(5)	0.2939(3)	0.0569(2)	0.0446(7)
C(7)	−0.2261(5)	0.2099(3)	0.1600(2)	0.0366(7)
C(8)	−0.3716(5)	0.1850(3)	0.2271(2)	0.0436(7)
C(9)	−0.3534(5)	0.1016(3)	0.2892(2)	0.0457(8)
C(10)	−0.1861(5)	0.0397(3)	0.2866(2)	0.0420(8)
C(11)	−0.0398(5)	0.0605(3)	0.2210(2)	0.0434(7)
C(12)	−0.0603(5)	0.1454(3)	0.1586(2)	0.0415(8)
O(13)	−0.1699(4)	−0.0411(2)	0.3514(2)	0.0555(7)
C(14)	−0.1589(5)	0.4434(3)	0.1561(2)	0.0376(7)
C(15)	0.0525(5)	0.4773(3)	0.2015(2)	0.0463(7)
C(16)	0.1373(5)	0.5936(3)	0.2542(2)	0.0459(7)
C(17)	0.0096(5)	0.6799(3)	0.2632(2)	0.0435(8)
C(18)	−0.1999(5)	0.6502(3)	0.2203(2)	0.0491(7)
C(19)	−0.2815(5)	0.5337(3)	0.1670(2)	0.0464(7)
O(20)	0.0861(4)	0.7979(2)	0.3143(2)	0.0580(7)
O(21)	−0.5383(4)	−0.1681(2)	0.4181(2)	0.0709(6)
C(22)	−0.5105(5)	−0.2445(3)	0.4851(2)	0.0535(8)
C(23)	−0.3052(5)	−0.2369(3)	0.5270(2)	0.0620(8)
C(24)	−0.2870(6)	−0.3159(4)	0.5932(3)	0.0702(8)
C(25)	−0.4714(7)	−0.4004(4)	0.6157(3)	0.0715(7)
C(26)	−0.6742(6)	−0.4059(3)	0.5752(3)	0.0700(8)
C(27)	−0.6966(5)	−0.3277(3)	0.5084(2)	0.0623(8)
H(13)	−0.0338	−0.0832	0.3434	0.050
H(20)	0.2461	0.8049	0.3461	0.050
H(21)	−0.3819	−0.1185	0.3986	0.050

organization in the complexes of **5** with *o*-cresol, *m*-cresol and *p*-cresol. Relevant geometric details of specific interactions are also included in Table VII.

The selective properties of host **5** upon complexation with the different guest moieties are reflected in the results of crystallization studies from a three-component mixture (two guests + host) in ethylacetate. The following guest ratios were detected by gas chromatography in material obtained by crystallization of **5** in the presence of a 1 : 1 mixture of two cresols or cresol and phenol: phenol–*o*-cresol 57.3 : 42.7; phenol–*p*-cresol 45.7 : 54.3; *o*-cresol–*p*-cresol 35.2 : 64.8; *o*-cresol–*m*-cresol 26.2 : 73.8; *m*-cresol–*p*-cresol 65.9 : 34.1.

4. Discussion

As will be shown below the structural results correlate well with the observed tendency of host **5** to prefer complexation with one phenol derivative over another. In view of the isomorphicity of the four structures the different guest components

Table VI. Comparison of Bond Lengths (Å) and Bond Angles (deg.)

Bond	I	II	III	IV
C(1)—C(2)	1.517(16)	1.548(4)	1.543(4)	1.542(4)
C(1)—C(6)	1.563(16)	1.546(3)	1.532(4)	1.534(4)
C(1)—C(7)	1.557(16)	1.544(4)	1.539(5)	1.539(4)
C(1)—C(14)	1.531(14)	1.531(3)	1.538(4)	1.533(4)
C(2)—C(3)	1.537(14)	1.526(3)	1.523(4)	1.531(4)
C(3)—C(4)	1.548(16)	1.529(4)	1.519(5)	1.508(4)
C(4)—C(5)	1.496(17)	1.517(4)	1.515(5)	1.513(4)
C(5)—C(6)	1.543(14)	1.529(3)	1.519(4)	1.523(4)
C(7)—C(8)	1.362(16)	1.392(4)	1.379(4)	1.389(4)
C(7)—C(12)	1.372(17)	1.389(3)	1.389(5)	1.384(5)
C(8)—C(9)	1.396(16)	1.380(4)	1.382(5)	1.373(4)
C(9)—C(10)	1.374(17)	1.378(4)	1.362(5)	1.373(5)
C(10)—C(11)	1.354(16)	1.373(4)	1.370(4)	1.371(4)
C(10)—O(13)	1.398(13)	1.387(3)	1.386(4)	1.380(4)
C(11)—C(12)	1.406(15)	1.392(4)	1.380(5)	1.391(4)
C(14)—C(15)	1.390(15)	1.396(3)	1.386(4)	1.389(4)
C(14)—C(19)	1.372(17)	1.387(4)	1.380(5)	1.387(5)
C(15)—C(16)	1.385(14)	1.382(3)	1.376(4)	1.381(4)
C(16)—C(17)	1.364(18)	1.380(4)	1.374(5)	1.373(5)
C(17)—C(18)	1.377(16)	1.384(3)	1.378(5)	1.365(4)
C(17)—O(20)	1.406(12)	1.374(2)	1.378(3)	1.380(3)
C(18)—C(19)	1.402(14)	1.386(4)	1.387(4)	1.385(4)
O(21)—C(22)	1.389(11)	1.381(3)	1.376(4)	1.386(4)
C(22)—C(23)	1.395	1.380(3)	1.364(5)	1.368(4)
C(22)—C(27)	1.395	1.375(4)	1.372(4)	1.368(4)
C(23)—C(24)	1.395	1.379(4)	1.387(7)	1.384(5)
C(24)—C(25)	1.395	1.376(4)	1.366(5)	1.364(5)
C(25)—C(26)	1.395	1.383(4)	1.375(6)	1.351(5)
C(26)—C(27)	1.395	1.386(4)	1.376(6)	1.390(5)

The C—Me bond lengths in the various derivatives of cresol are: **I**. C(27)—C(28) 1.424(15); **II**. C(26)—C(28) 1.503(4); **III**. C(25)—C(28) 1.509(6) Å. The phenyl ring of *o*-cresol in **I** was refined with a constrained geometry.

Angle	I	II	III	IV
C(7)—C(1)—C(14)	106.1(9)	107.2(2)	107.1(3)	107.0(2)
C(6)—C(1)—C(14)	111.2(9)	111.9(2)	111.4(3)	111.1(3)
C(6)—C(1)—C(7)	109.5(9)	110.3(2)	110.9(3)	110.9(3)
C(2)—C(1)—C(14)	108.9(9)	108.7(2)	108.5(3)	109.1(3)
C(2)—C(1)—C(7)	113.3(9)	112.7(2)	112.9(3)	112.8(3)
C(2)—C(1)—C(6)	107.8(9)	106.2(2)	106.1(3)	106.0(2)
C(1)—C(2)—C(3)	114.8(9)	114.4(2)	113.7(3)	114.3(3)
C(2)—C(3)—C(4)	110.2(9)	111.2(3)	111.9(3)	111.2(3)
C(3)—C(4)—C(5)	111.6(10)	111.0(3)	110.1(3)	110.5(3)
C(4)—C(5)—C(6)	111.7(10)	110.9(2)	111.2(4)	111.4(3)
C(1)—C(6)—C(5)	111.0(9)	112.7(2)	113.2(3)	112.7(3)
C(1)—C(7)—C(12)	121.7(10)	123.2(2)	123.1(3)	123.5(3)
C(1)—C(7)—C(8)	120.0(10)	119.7(2)	120.8(3)	120.0(3)
C(8)—C(7)—C(12)	118.1(10)	116.9(2)	116.0(3)	116.3(3)
C(7)—C(8)—C(9)	123.3(11)	122.3(3)	122.7(4)	122.4(3)
C(8)—C(9)—C(10)	116.6(10)	119.2(3)	119.6(3)	120.0(3)
C(9)—C(10)—O(13)	121.6(11)	117.6(3)	122.2(4)	118.3(3)

Table VI (contd.)

Angle	I	II	III	IV
C(9)—C(10)—C(11)	122.2(10)	120.4(2)	119.9(3)	119.6(3)
C(11)—C(10)—O(13)	116.2(11)	122.0(3)	118.0(4)	122.1(3)
C(10)—C(11)—C(12)	119.4(11)	119.7(3)	119.8(4)	119.7(3)
C(7)—C(12)—C(11)	120.3(11)	121.5(3)	122.1(4)	122.0(3)
C(1)—C(14)—C(19)	123.1(10)	123.7(2)	123.8(3)	124.3(3)
C(1)—C(14)—C(15)	119.6(10)	119.9(2)	119.9(3)	119.9(3)
C(15)—C(14)—C(19)	117.3(10)	116.4(3)	116.3(3)	115.9(3)
C(14)—C(15)—C(16)	121.3(11)	122.5(3)	122.6(4)	122.5(3)
C(15)—C(16)—C(17)	120.2(11)	119.6(3)	120.0(4)	119.6(3)
C(16)—C(17)—O(20)	118.1(11)	122.4(3)	118.9(4)	122.1(3)
C(16)—C(17)—C(18)	120.4(11)	119.5(3)	118.9(3)	119.9(3)
C(18)—C(17)—O(20)	121.5(11)	118.1(3)	122.1(4)	118.0(3)
C(17)—C(18)—C(19)	118.6(11)	120.0(3)	120.1(4)	119.8(3)
C(14)—C(19)—C(18)	122.2(11)	122.0(3)	122.0(4)	122.4(3)
O(21)—C(22)—C(27)	119.6(8)	117.7(3)	121.8(3)	117.5(3)
O(21)—C(22)—C(23)	120.4(8)	120.9(3)	118.7(3)	121.5(3)
C(23)—C(22)—C(27)	120.0	121.4(3)	119.6(4)	121.0(3)
C(22)—C(23)—C(24)	120.0	118.3(3)	119.8(4)	119.0(3)
C(23)—C(24)—C(25)	120.0	120.7(3)	121.7(4)	120.2(4)
C(24)—C(25)—C(26)	120.0	121.1(3)	117.2(4)	120.5(4)
C(25)—C(26)—C(27)	120.0	118.1(3)	122.0(4)	120.3(4)
C(22)—C(27)—C(26)	120.0	120.4(3)	119.6(4)	118.9(3)

The C—C—Me bond angles in the various derivatives of cresol are: **I**. C(26)—C(27)—C(28) 118.3(9), C(22)—C(27)—C(28) 121.6(9); **II**. C(25)—C(26)—C(28) 121.2(3), C(27)—C(26)—C(28) 120.7(3); **III**. C(24)—C(25)—C(28) 122.4(5), C(26)—C(25)—C(28) 120.4(4)°.

are located in a similar crystalline environment, and it becomes possible to assess the effect of individual interactions on the relative stability of the entire system.

The crystallographic analysis leads to the following generalizations. All four structures are characterized by an almost identical intermolecular organizations with the same general pattern of hydrogen bonds and van der Waals interactions. Every hydroxyl group in the structure is involved in two hydrogen bonds, acting simultaneously as a proton donor to one site and as a proton acceptor from another site. The geometries of the nearly linear H-bonds indicate strong interaction, the OH ··· O distances ranging from 2.65 to 2.70 Å in **II**, **III** and **IV** (Table VII). In complex **I** two of the bonds are slightly less effective (2.73 and 2.74 Å) as a result of a severe steric hindrance present in this structure (see below). The stability of the hydrogen-bonding pattern is further reflected in the rather small variation of the *a* (from 6.232 to 6.270 Å) and *b* (from 10.807 to 10.907 Å) dimensions and of the inter-axial angles in the four crystals (Table I).

It is considerably easier, however, to induce an expansion of the periodicity along *c*, since along this axis the 'layered' structure is stabilized mainly by weaker dispersion forces. Indeed, the structural variation of the guest species caused a significant increase of the *c*-axis from 14.845 Å in **IV** through 15.490 Å in **II** to 15.818 Å in **III** in order to accommodate the additional methyl substituent. The relative orientation of the guest phenyl ring with respect to the surrounding host moieties, and the overlap between adjacent guests related to each other by inversion at the center of the

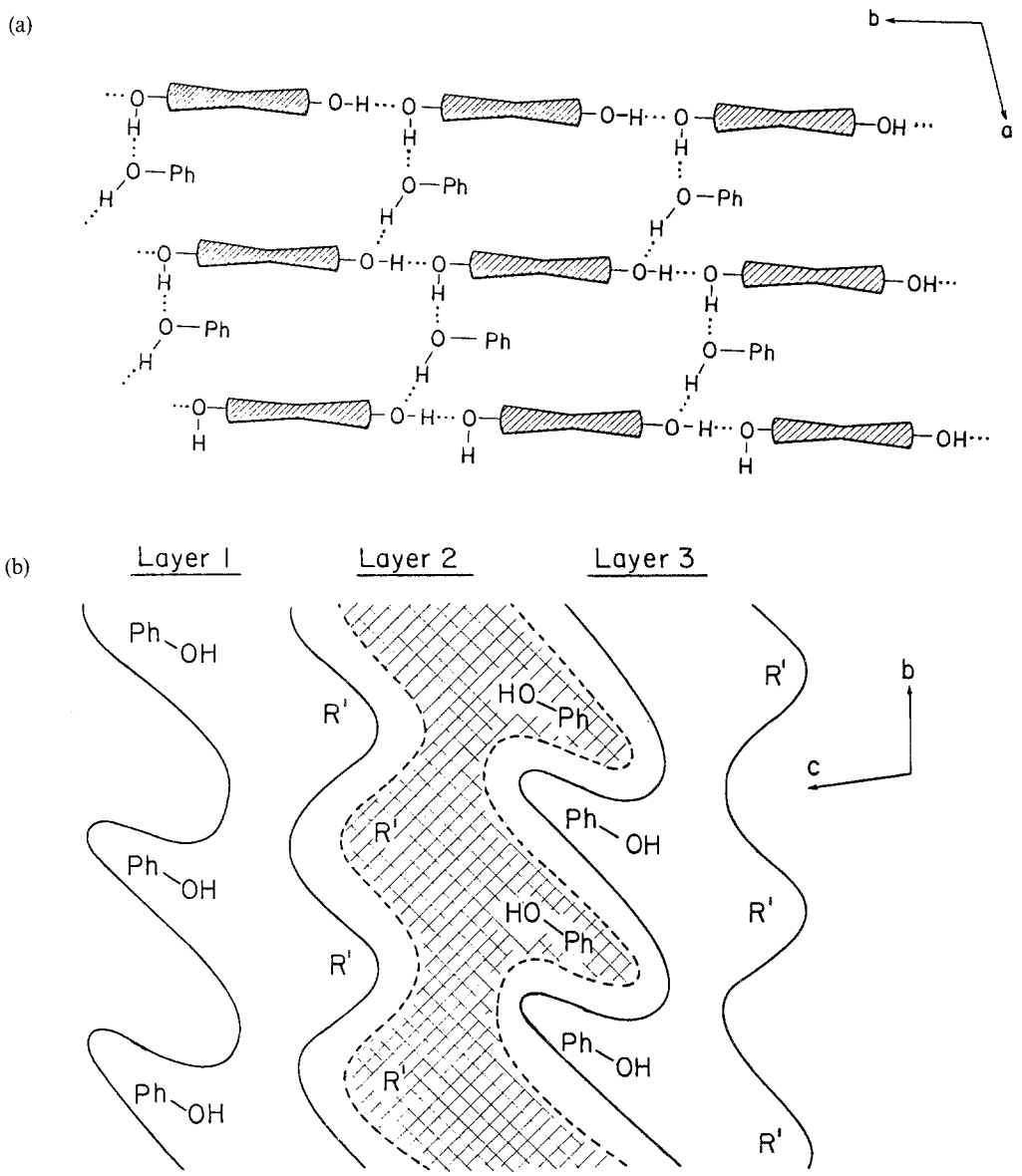

Fig. 2. A general schematic illustration of the structural model: (a) The two-dimensional hydrogen bonding pattern parallel to *ab*; the shaded areas represent the 1,1-diphenylcyclohexane framework. (b) The van der Waals type packing of the hydrogen-bonded layers along the *c*-axis; R′ represents the cyclohexyl ends of the host species.

unit-cell, can also be varied to some extent, thus providing another parameter of structural flexibility.

The four structures are characterized by a similar packing pattern along the cyclohexyl sides of the H-bonded layers. The shortest distance between adjacent layers is represented by the C(3)···C(17) interaction. The values vary from 3.672 to 3.747 Å, in good agreement with a van der Waals distance of about 3.7 Å expected between phenyl and methylene carbon atoms. On the other side of the layer the guest

Table VII. Relevant Structural Parameters of Intermolecular Interactions

(a) Geometry of the hydrogen bonds

Donor (OH)	Acceptor (O)	O—H (Å)	O···O (Å)	H···O (Å)	O—H···O (deg.)
Compound **I***					
OH(13)	O(21)	1.01	2.742(11)	1.83	148
OH(20)	O(13)	1.05	2.696(12)	1.78	143
OH(21)	O(20)	0.95	2.732(11)	1.81	162
Compound **II**					
OH(13)	O(20)	1.02	2.702(3)	1.70	165
OH(20)	O(21)	0.99	2.675(3)	1.70	166
OH(21)	O(13)	1.06	2.703(3)	1.65	177
Compound **III**					
OH(13)	O(21)	1.01	2.676(4)	1.68	167
OH(20)	O(13)	1.08	2.660(4)	1.60	166
OH(21)	O(20)	1.07	2.696(4)	1.63	171
Compound **IV**					
OH(13)	O(20)	1.06	2.682(4)	1.68	155
OH(20)	O(21)	1.06	2.648(4)	1.61	164
OH(21)	O(13)	1.06	2.671(4)	1.62	169

* The positions of the H-atoms in **I** are not reliable.

(b) Selected nonbonding distances reflecting on intermolecular van der Waals interactions

Compound **I**

C(3)···C(17) at −x, 1−y, −z	3.708 Å
C(25)···C(8) at −1−x, −y, 1−z	3.598
C(28)···C(28) at −x, −y, 1−z	3.505

Compound **II**

C(3)···C(17) at −x, 1−y, −z	3.732 Å
C(24)···C(10) at −x, −y, 1−z	3.514
C(26)···C(9) at −1−x, −y, 1−z	3.498
C(28)···C(8) at −1−x, −y, 1−z	3.698
C(28)···C(17) at −1−x, −y, 1−z	3.743
C(28)···C(25) at −1−x, −1−y, 1−z	3.704

Compound **III**

C(3)···C(17) at −x, 1−y, −z	3.747 Å
C(25)···C(9) at −1−x, −y, 1−z	3.500
C(26)···C(9) at −1−x, −y, 1−z	3.525
C(28)···C(8) at −1−x, −y, 1−z	3.578
C(28)···C(19) at −1−x, −y, 1−z	3.698
C(28)···C(26) at −1−x, −1−y, 1−z	3.683

Compound **IV**

C(3)···C(17) at −x, 1−y, −z	3.672 Å
C(25)···C(8) at −1−x, −y, 1−z	3.492
C(26)···C(8) at −1−x, −y, 1−z	3.550

The average e.s.d.'s are 0.016 Å in **I**, and 0.005 Å in **II–IV**

Table VII (contd.)

(c) Interplanar distances between the partially overlapping quests related to each other by inversion at $\frac{1}{2},\frac{1}{2},\frac{1}{2}$

(**I**) 3.92 Å; (**II**) 3.55 Å; (**III**) 3.63 Å; (**IV**) 3.59 Å

(d) Dihedral angles (deg) between planes of the three phenyl rings

Plane (1) through atoms C(7) -to-C(12),
Plane (2) through atoms C(14)-to-C(19),
Plane (3) through atoms C(22)-to-C(27).

Compound:	**I**	**II**	**III**	**IV**
Planes (1) and (2)	85.1	87.5	88.2	88.9
Planes (1) and (3)	57.5	48.9	42.0	44.0
Planes (2) and (3)	70.1	67.5	64.6	68.7

phenyl ring in each structure is located between another guest moiety (located across the $\frac{1}{2},\frac{1}{2},\frac{1}{2}$ center of inversion) and the C(7)-through-C(12) ring of host molecules of an adjacent layer. Since the normal to these planes extends roughly parallel to the *b*-axis which is fixed by the H-bonding pattern, a steric misfit between them will have a noticeable effect on the balance between attractive and repulsive forces in the structure.

It is possible to detail some significant differences between modes of van der Waals

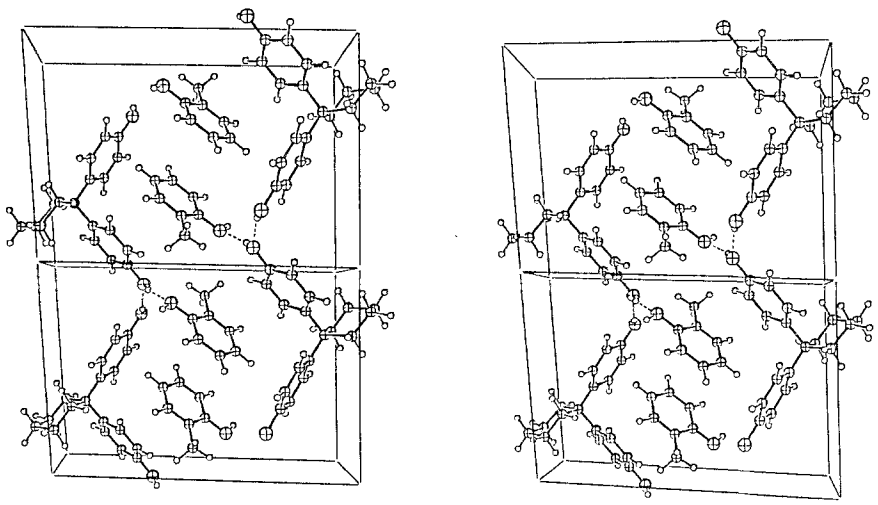

Fig. 3. Stereoview of the crystal structure of complex **I**, approximately down the *a*-axis (*c* is horizontal).

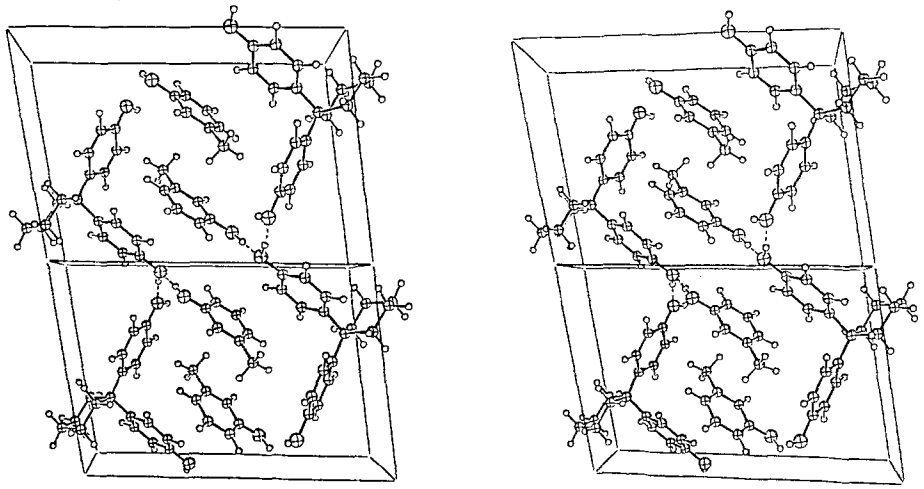

Fig. 4. Stereoview of the crystal structure of complex **II**, approximately down the *a*-axis (*c* is horizontal).

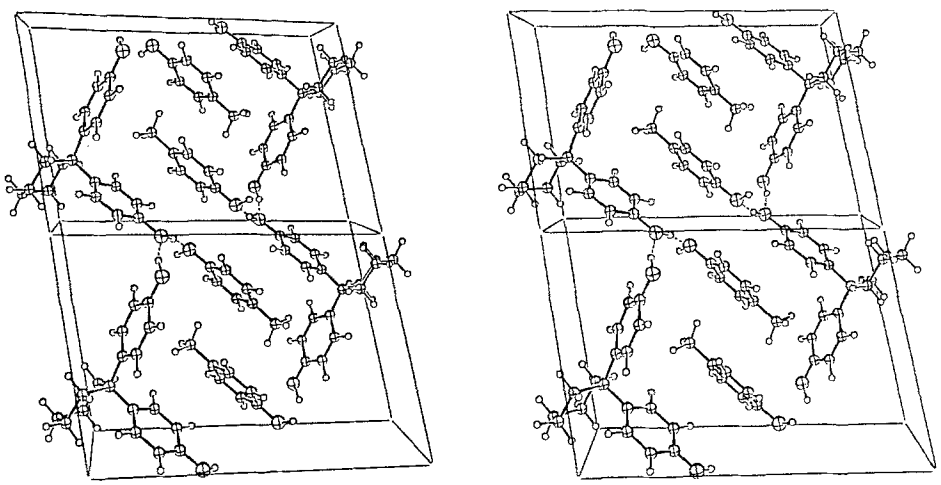

Fig. 5. Stereoview of the crystal structure of complex **III**, approximately down the *a*-axis (*c* is horizontal).

interactions in the four crystal structures by surveying the list of relevant intermolecular distances given in Table VII. Ordinary nonbonding distances characterize structure **IV** containing the unsubstituted phenyl as guest. Shortest contacts involve adjacent phenyl rings with C···C distances of 3.5–3.6 Å, well within range of characteristic van der Waals values [7]. The substitution of a methyl group on the guest species contributes additional interactions. In fact, as can be anticipated from the schematic illustration in Figure 2a, the guest phenyls in **IV** are rather loosely packed along the *a*-axis of the crystal; all relevant intermolecular distances are $\geqslant 4.0$ Å. Correspondingly, replacement of the phenol by *m*-cresol (with the methyl oriented partially along *a*) is associated with an increase of only about 0.65 Å in the length of the *c*-axis in **II**. The additional methyl is perfectly well accommodated within the expanded lattice without an apparent distortion of the other interactions; the guest phenyl moiety and the methyl substituent are located at 3.50–3.55 Å and

3.70–3.74 Å respectively from their surroundings (adjacent phenyl 'walls'), as is normally expected [7].

A substitution of the methyl group in the *para* position (a peripheral site of each layer) causes an additional expansion of the unit-cell along *c* in **III**. The crystal packing of the resulting structure is still an efficient one with phenyl ··· phenyl nonbonding distances within the range 3.50–3.63 Å. However, the para-substituted methyl introduces already some steric hindrance into the structure. This is illustrated by the relatively short approach C(28) ··· C(8) of 3.578 Å (Table VII), as compared to the normal van der Waals methyl ··· phenyl distance of about 3.7 Å. The latter is observed with respect to the two other phenyl rings in **III** (3.68–3.70 Å) as well as in structure **II**. This steric misfit could be responsible for the preferential complexation of host **5** with *m*-cresol rather than with *p*-cresol (see above).

Clearly, complex **I** forms the least stable structure. Introduction of the methyl substituent at the *ortho* position has an unfavourable effect on the intermolecular arrangement. In the observed structure, which is primarily determined by hydrogen-bonding interactions, the CH_3 groups of guest molecules interrelated by inversion at 0, 0, $\frac{1}{2}$ essentially collide one into the other. The corresponding observed methyl ··· methyl distance is 3.505 Å, about 0.5 Å (!) shorther than the sum of van der Waals radii [7]. Moreover, the π–π interaction between the partially overlapping guests located around the $\frac{1}{2}, \frac{1}{2}, \frac{1}{2}$ center of inversion is considerably reduced in this structure; the interplanar distance has increased from about 3.6 Å in the previous examples to 3.92 Å here (Table VII). The inefficient crystal packing of the molecular entities in **I** makes this structure relatively unstable due to poor interactions between the hydrogen bonded layers. This is consistent with the observed slow deterioration of the crystals at room temperature.

The above results confirm that an inclusion-type crystallization is an excellent technique for molecular separation between species of nearly identical chemical and physical properties but containing a small structural variation. In such case it can reasonably be assumed that the solvation effects before crystallization are similar in all structures. On the other hand, the crystalline state represents a close-packed phase, and its relative stability is very sensitive to the degree of spatial and functional complementarity between the various constituents. Preferential complexation of a suitable host with one guest out of a mixture of two or more structural analogues is in fact determined mainly by differences in these features of complementarity. The evaluation of structural results presented in this account awaits further confrontation with quantitative estimates of the intermolecular interactions by appropriate theoretical calculations.

References

1. F. Toda, K. Tanaka, G. U. Daumas, and M. C. Sanchez: *Chem. Lett.* **1983**, 1521;
F. Toda, K. Tanaka, Y. Tagami, and T. C. W. Mak: *Chem. Lett.* **1985**, 195;
F. Toda, K. Tanaka, and T. C. W. Mak: *Bull. Chem. Soc. Jpn.* **58**, 2221 (1985);
F. Toda, K. Tanaka, Y. Wang, and G.-H. Lee: *Chem. Lett.* **1986**, 109;
F. Toda, Y. Tagami, and T. C. W. Mak: *Bull. Chem. Soc. Jpn.* **59**, 1189 (1986), and *Chem. Lett.* **1986**, 1909;
K. Dohi, K. Tanaka, and F. Toda: *J. Chem. Soc. Jpn.* **1986**, 927;
K. Tanaka and F. Toda: *J. Chem. Soc. Jpn.* **1986**, 932.
2. E. Weber, I. Csoregh, B. Stensland, and M. Czugler: *J. Am. Chem. Soc.* **106**, 3297 (1984);
M. Czugler, J. G. Angyan, G. Naray-Szabo, and E. Weber: *J. Am. Chem. Soc.* **108**, 1275 (1986).

3. H. Hart, L.-T. W. Lin, and D. L. Ward: *J. Chem. Soc. Chem. Commun.* **1984**, 293;
H. Hart, L.-T. W. Lin and I. Goldberg: *J. Incl. Phenom.* **2**, 377 (1984) and *Mol. Cryst. Liq. Cryst.* **137**, 277 (1986).
4. M. E. McGreal, V. Niederl, and J. B. Niederl: *J. Am. Chem. Soc.* **61**, 345 (1939); although this compound was known for a long time its inclusion ability has been discovered by the Japanese authors (K. T. and F. T.) only recently.
5. P. Main, S. J. Fiske, S. E. Hull, L. Lessinger, G. Germain, J. P. Declercq, and M. M. Woolfson: MULTAN 80. A System of Computer Programs for the Automatic Solution of Crystal Structures from X-ray Diffraction Data. Univs. of York, England and Louvain, Belgium (1980).
6. G. M. Sheldrick: SHELX 76. Program for Crystal Structure Determination, Univ. of Cambridge, England (1976).
7. L. Pauling: in *The Nature of the Chemical Bond*, New York, Cornell University Press (1960).